ChemElectroChem

Research Article
doi.org/10.1002/celc.202300753

Chemistry Europe
European Chemical Societies Publishing

www.chemelectrochem.org

Electrochemical Ethanol Oxidation using RuO_2-Based Catalysts: Suppressing OER and Tailored Switching between Water Oxidation and Ethanol Oxidation

Ina Kohlhaas,[a] Nils Kurig,[a] and Regina Palkovits*[a, b]

For an efficient hydrogen production, electrochemical ethanol oxidation is a great alternative to the oxygen evolution reaction (OER) due to the generation of value-added products. In this electrosynthetic contribution, the properties of ethanol oxidation are investigated with regard to the influence of pH, temperature and potential using RuO_2-based catalysts. Results show acetic acid as main reaction product with yields of up to 29% and Faraday efficiencies of $\geq$71%. Increasing the potential marginally from 1.40 V vs. RHE to 1.45 V vs. RHE promoted parasitic OER and, therefore, yield ($\geq$10%) and Faraday efficiency ($\geq$56%) of the organic products decreased. Doping RuO_2 electrodes with TiO_2 shows promising results in suppressing OER during ethanol oxidation. Additionally, the catalyst allows moderate OER potentials in water electrolysis, making the catalyst a switchable material.

Introduction

Global warming has led to a change in our look on fossil energy sources within the last few decades. Alternative energy resources like wind, water, or solar energy enable emission-free power production but undergo daily, seasonal, and location-dependent fluctuations. To make those renewable energy sources applicable to daily needs, storage and alternative application methods must be found.[1] H_2 is now an often considered opportunity to store energy utilizing electrochemical water splitting.[2–4] Currently, the oxygen evolution reaction (OER) is the main challenge in achieving an economical process due its high thermodynamic potential of 1.23 V vs. reversible hydrogen electrode (RHE) and the low commercial value of oxygen.[4,5] Coupling hydrogen evolution reaction (HER) with alternative anode reactions, like ethanol oxidation, with lower thermodynamic potentials could increase the economic value of the reaction.[5,6] Furthermore, ethanol can be derived from biomass by hydrolysis of carbohydrate polymers and subsequent fermentation and thus represents a sustainable substrate.[2,7] Products of electrochemical ethanol oxidation are acetaldehyde, acetic acid, and CO_2.[8]

Many publications have reported a wide variety of catalyst materials for electrochemical ethanol oxidation.[9,10] Most are based on Pt and Pd.[9,10,11] Pt is used in ethanol oxidation due to its high stability in organic media as well as its ability to catalyze both oxidation and C–C bond cleavage mechanisms, respectively.[12] Pd shows a high selectivity towards oxidation mechanisms. In addition to its intrinsic catalytic activity, Pd was observed to enhance the performance of other metallic elements due to synergic effects.[9] The selectivity towards C_2-products is usually increased by formation of bimetallic alloys which in addition also show improved resistance towards CO poisoning seen for pure Pt and Pd.[13] Here, many combinations using precious and non-precious metals are reported in literature spanning from Ru and Rh to Ni and Sn.[9,13] Alloy nanoparticles are usually deposited onto support materials like carbon, TiO_2 or SnO_2 providing high stability of the system and decreasing cost compared to pure alloy catalysts.[9,14] In this research, we utilized TiO_2 doped RuO_2 on Ti. RuO_2 is widely known as a catalyst with high electrochemical activity, corrosion resistance and thermal stability.[15–18] It is a popular catalyst in the chloralkali industry and a benchmark for OER activity in acidic water splitting.[15–17] The addition of RuO_2 to catalysts for electrochemical alcohol oxidation was shown to promote CO removal from the catalyst surface due to its oxophilic characteristics.[17,19,20] Shieh *et al.* and Kim *et al.* reported cyclic voltammetry (CV) studies of RuO_2 on Ti and Ni sheets proving the activity for ethanol oxidation under mild reaction conditions.[16] Recently, Tian *et al.* developed a vacancy rich $IrRuO_x$ catalyst which showed highly promising results for ethanol oxidation reaching acetic acid generation rates of up to 30 $mmol \cdot cm^{-2} \cdot h^{-1}$ at current densities of 3 $A \cdot cm^{-2}$.[21] Aside from Ir, TiO_2 was reported as dopant in RuO_2-based compound materials.[22] TiO_2 is a popular support in heterogenous catalysis because of its high chemical inertness and stability.[15,19,23] Its

[a] I. Kohlhaas, Dr. N. Kurig, Prof. Dr. R. Palkovits
Institut für Technische und Makromolekulare Chemie
RWTH Aachen University
Worringerweg 2, 52074 Aachen (Germany)
E-mail: palkovits@itmc.rwth-aachen.de

[b] Prof. Dr. R. Palkovits
Institute for a Sustainable Hydrogen Economy
Forschungszentrum Jülich
Am Brainenergy Park 4, 52428 Jülich (Germany)
E-mail: r.palkovits@fz-juelich.de

Supporting information for this article is available on the WWW under https://doi.org/10.1002/celc.202300753

activity in ethanol oxidation was reported before using photochemistry.[24]

While current literature in electrochemical ethanol oxidation oftentimes focuses on the development of novel catalyst materials and their characterization, this contribution focusses on practical application of ethanol oxidation in electrosynthesis. Here, the effect of TiO_2-doping of RuO_2 for electrochemical ethanol oxidation was investigated to tune the selectivity for ethanol oxidation over OER. Pt and RuO_2-based materials are applied as catalysts because they are well established in the field. In addition, RuO_2 acts as a benchmark catalyst for OER enabling comparison between OER and ethanol oxidation.

Results and Discussion

First, ethanol oxidation and OER were investigated using cyclic voltammetry to determine reaction potentials for electrolysis experiments (details are available in the supporting information, Figure S 3–7). TiO_2 shows no activity in ethanol oxidation and low OER activity in either H_2SO_4 or KOH. However, both Pt and RuO_2 possess activity in ethanol oxidation at potentials below OER in ethanol-containing electrolyte solution, as the OER potential is shifted to higher potentials in the presence of ethanol. It should be noted that the use of RuO_2 results in similar reaction potentials of around 1.4 V vs. RHE in both alkaline and acidic electrolyte solution, while the potential using Pt increases from 1.72 V vs. RHE to 2.1 V vs. RHE in alkaline solution.

Additionally, the materials were electrochemically characterized to increase material understanding and to gain further mechanistic insight. Electrochemical impedance spectroscopy (EIS) (Figure 1) was conducted and Tafel slope as well as double layer capacitance (C_{dl}) were calculated from voltammetry data (Figure 3). RuO_2-based materials were analyzed regarding OER and ethanol oxidation in both acidic and alkaline electrolyte solution at room temperature. EIS measurements of OER (Figure 1a,b) show an increase in charge transfer resistance (R_{ct}) with increasing TiO_2 content that can be explained by the high resistance of semiconductors, decreasing the overall conductivity of the electrode.[24] Similar R_{ct} values of between 0.2 Ω, and 0.9 Ω for $(Ru_{0.5}:Ti_{0.5})O_2$, $(Ru_{0.75}:Ti_{0.25})O_2$ and RuO_2 were obtained in alkaline and acidic electrolyte solution. The same trend could be observed during the investigation of ethanol oxidation (Figure 1c,d), here R_{ct} values between 0.4 Ω and 1.1 Ω were obtained for respective catalysts. Tafel slopes (Figure 2a–d) for the investigated catalyst systems were calculated taking the internal resistance R_i of the system into account. All electrodes show a dual Tafel character for OER in both acidic and alkaline electrolyte media (Figure 2 a,b). Values of 80 mV·dec^{-1}, 95 mV·dec^{-1} and 89 mV·dec^{-1} were observed in the low Tafel region for RuO_2, $(Ru_{0.75}:Ti_{0.25})O_2$ and $(Ru_{0.5}:Ti_{0.5})O_2$ in 1 M KOH. Values for the high Tafel region reached from 114 mV·dec^{-1} to 214 mV·dec^{-1} and 374 mV·dec^{-1} for the respective catalysts. In 1 M H_2SO_4, the values of the low Tafel region reached from 103 mV·dec^{-1} to 68 mV·dec^{-1} and 85 mV·dec^{-1} for RuO_2, $(Ru_{0.75}:Ti_{0.25})O_2$ and $(Ru_{0.5}:Ti_{0.5})O_2$, respectively. In high Tafel regions, the values spanned between 273 mV·dec^{-1}, 126 mV·dec^{-1} and 348 mV·dec^{-1} for the respective catalysts. These changes in Tafel slope observed for both electrolyte systems, i.e., pH regimes, can be attributed to mass transport limitation due to increasing gas evolution at high potentials causing a decrease in effective surface area of the electrode. However, a dual mechanistic behavior of the catalyst with a change of the rate determining step as reported for other catalyst systems cannot be observed as no clear agreement in potential for the change can be observed.[25] For ethanol oxidation (Figure 2 c,d) only the initial phase after the onset potential was analyzed using Tafel plot because with increasing potential a mix between ethanol oxidation and OER can be

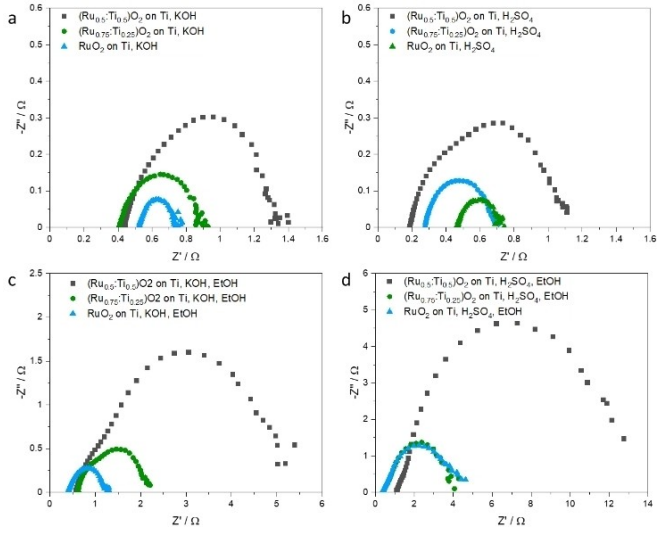

Figure 1. Electrochemical impedance spectroscopy using RuO_2 on Ti, $(Ru_{0.75}:Ti_{0.25})O_2$ on Ti and $(Ru_{0.5}:Ti_{0.5})O_2$ on Ti at room temperature a) in 1 M KOH, b) in 1 M H_2SO_4, c) in 1 M KOH with 0.1 M ethanol d) in 1 M H_2SO_4 with 0.1 M ethanol.

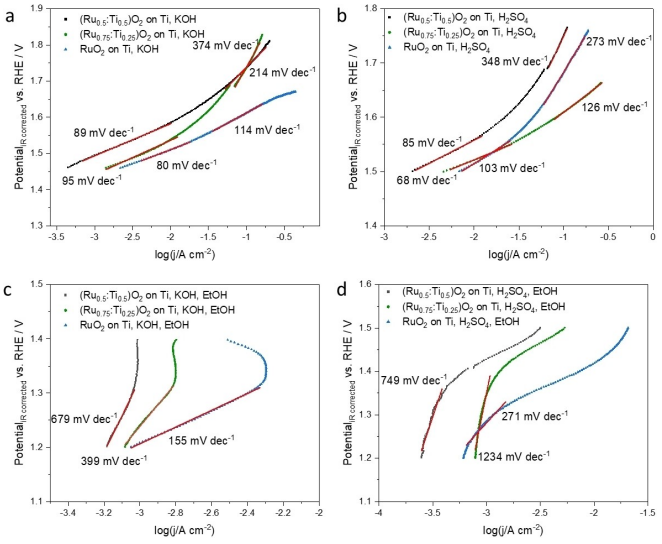

Figure 2. Tafel plot using RuO_2 on Ti, $(Ru_{0.75}:Ti_{0.25})O_2$ on Ti and $(Ru_{0.5}:Ti_{0.5})O_2$ on Ti at room temperature a) in 1 M KOH, b) in 1 M H_2SO_4, c) in 1 M KOH with 0.1 M ethanol d) in 1 M H_2SO_4 with 0.1 M ethanol.

observed, making Tafel analysis increasingly complex. In 1 M KOH Tafel slopes increased from 155 mV·dec^{-1} to 399 mV·dec^{-1} and 679 mV·dec^{-1} from RuO_2 to $(Ru_{0.5}:Ti_{0.5})O_2$. In 1 M H_2SO_4 values spanned from 271 mV·dec^{-1} to 1234 mV·dec^{-1} and 749 mV·dec^{-1} for the respective catalysts. Interestingly, no clear correlation between neither TiO_2 nor RuO_2 amount and change in Tafel slope can be determined, making Tafel analysis insufficient to analyze interaction between the catalyst compounds. C_{dl} was determined by plotting the average current in non-faradaic regions over the scan rate and calculating the slope (Figure 3a–d). OER results (Figure 3a,b) show an increase from 16 mF·cm^{-2} to 61 mF·cm^{-2} in C_{dl} when reducing the amount of TiO_2 in the electrode material using 1 M KOH as electrolyte. A different effect was observed using H_2SO_4 as electrolyte. Here, the C_{dl} increased from 38 mF·cm^{-2} to 43 mF·cm^{-2} when increasing the amount of TiO_2 to 25% before decreasing to 24 mF·cm^{-2} at 50% TiO_2 content. The electrochemical surface area (ECSA) was calculated from the C_{dl} and the specific capacitance C_s. C_s was estimated to 35 µF·cm^{-2} in 1 M H_2SO_4 and 40 µF·cm^{-2} in 1 M KOH.[26] ECSA values in 1 M KOH range from 26 m^2·g^{-1} to 42 m^2·g^{-1} and 47 m^2·g^{-1} for $(Ru_{0.5}:Ti_{0.5})O_2$, $(Ru_{0.75}:Ti_{0.25})O_2$ and RuO_2, respectively. In 1 M H_2SO_4, values from 43 m^2·g^{-1} and 51 m^2·g^{-1} to 34 m^2·g^{-1} were reached.

For ethanol oxidation (Figure 3c,d) the same trends were observed in KOH and H_2SO_4. In both cases $(Ru_{0.75}:Ti_{0.25})O_2$ showed the highest C_{dl} at 54 mF·cm^{-2} and 34 mF·cm^{-2} in KOH and H_2SO_4 respectively. RuO_2 and $(Ru_{0.5}:Ti_{0.5})O_2$ reached values of 21 mF·cm^{-2}, 20 mF·cm^{-2}, 54 mF·cm^{-2} and 34 mF·cm^{-2}. ECSA were calculated to 36 m^2·g^{-1} for RuO_2, 56 m^2·g^{-1} for $(Ru_{0.75}:Ti_{0.25})O_2$ and 34 m^2·g^{-1} for $(Ru_{0.5}:Ti_{0.5})O_2$ respectively. In acidic solution, values of 27 m^2·g^{-1}, 40 m^2·g^{-1} and 35 m^2·g^{-1} were obtained for respective catalysts. Besides OER in 1 M KOH, all results indicate an ESCA optimum at 25% TiO_2 content. According to literature, this might be caused by TiO_2 leading to a better distribution of RuO_2 at small quantities in addition to facilitating ion transport and charging of the electrochemical double layer.[27]

As a starting point for electrosynthesis, the influence of pH on electrochemical ethanol oxidation was investigated using H_2SO_4 and KOH electrolyte solutions at room temperature (Figure 4). Electrolysis experiments were carried out repeatedly to ensure reproducibility and error bars display the standard deviation. During electrosynthesis using H_2SO_4 at room temperature over 3 h, all used catalysts show the formation of acetic acid as well as acetaldehyde. The reaction potentials were set to 1.42 V vs. RHE for RuO_2-based catalysts and 1.72 V vs. RHE for Pt according to the onset potentials of ethanol oxidation observed in the CV. F_{eq} (referred to acetic acid) varied between 0.06 and 0.16 as the reaction was conducted using a fixed reaction time, allowing for maximum yield between 6% and 16%. The highest yields of 18±7% for acetic acid and 7±2% of acetaldehyde are observed using RuO_2. In case of $(Ru_{0.75}:Ti_{0.25})O_2$, decreased yields of 8±0% of acetic acid and 4±0% of acetaldehyde are obtained. This matches general expectations as TiO_2 is added to reduce OER and not active in ethanol oxidation itself as shown in CV data (Figure S 5). This finding, however, contradicts the results of the ECSA determination which would assume an increase in yield using $(Ru_{0.75}:Ti_{0.25})O_2$ because of the higher electrochemically active surface area. Apparently, the increase in electrode conductivity overpowers the effect of possible improved RuO_2 distribution on the electrode surface, leading to increased yields with pure RuO_2, highlighting the importance of considering the interplay of counteracting effects. Using Pt results in low yields of 1±0% acetic acid and 2±1% acetaldehyde indicating low catalytic activity for ethanol oxidation in acidic solution in comparison to RuO_2-based

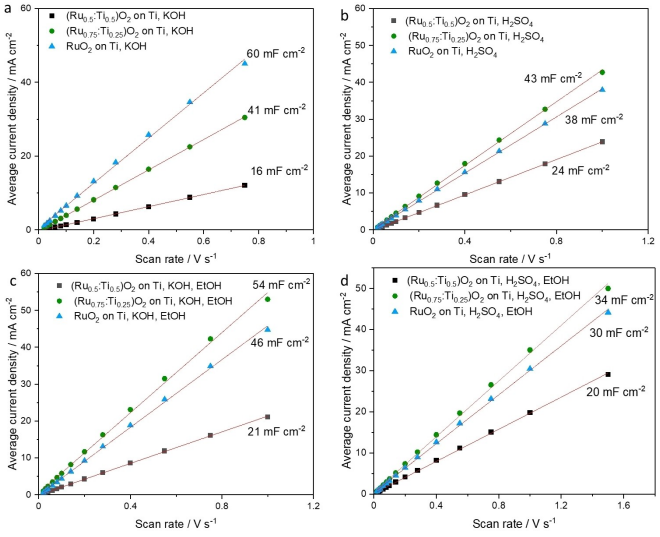

Figure 3. Double layer capacitance using RuO_2 on Ti, $(Ru_{0.75}:Ti_{0.25})O_2$ on Ti and $(Ru_{0.5}:Ti_{0.5})O_2$ on Ti at room temperature a) in 1 M KOH, b) in 1 M H_2SO_4, c) in 1 M KOH with 0.1 M ethanol d) in 1 M H_2SO_4 with 0.1 M ethanol.

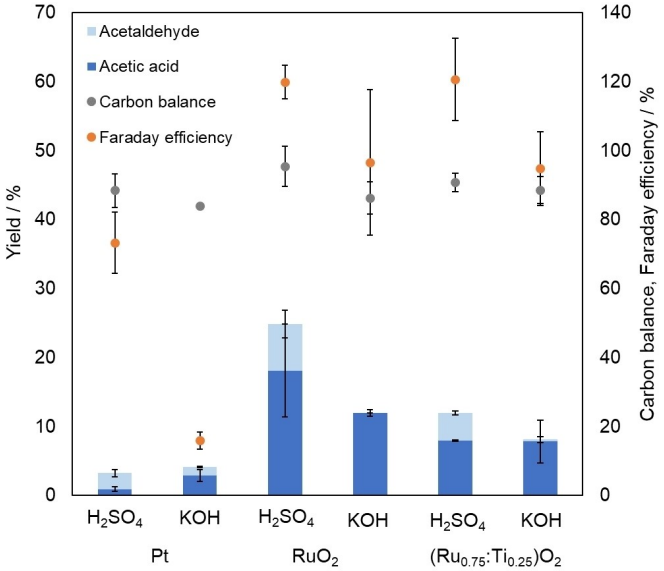

Figure 4. Yield, carbon balance and Faraday efficiency using Pt, RuO_2 on Ti and $(Ru_{0.75}:Ti_{0.25})O_2$ on Ti as catalyst for electrochemical ethanol oxidation of 0.1 M ethanol in 1 M H_2SO_4 or KOH. The reaction was conducted at room temperature for 3 h at a potential of 1.72 V vs. RHE (Pt, H_2SO_4), 1.42 V vs. RHE (RuO_2-based, H_2SO_4), 2.10 V vs. RHE (Pt, KOH). Applied potentials were determined prior according to the onset potential of ethanol oxidation.

catalysts. The carbon balance is similar for all used electrocatalysts (between 88±5% and 95±6%) and any gaps are due to formation of CO_2. While the electrolysis using Pt has a Faraday efficiency (*FE*) of 73±9%, implying side reactions like OER or CO_2 formation, both catalysts containing RuO_2 show a *FE* of around 121%. Therefore, blank experiments were performed to investigate possible non-electrochemical conversion of ethanol or acetaldehyde. The sample using ethanol without RuO_2 catalyst showed no formation of acetaldehyde or acetic acid. However, in case of acetaldehyde, low formation of acetic acid was observed without catalyst or current. Adding RuO_2 in powder form as catalyst, both ethanol and acetaldehyde showed some formation of oxidation products. These results indicate increased *FE* from alternative non-electrochemical pathways. These findings highlight the importance of performing actual electrosynthesis experiments as consecutive chemical reactions cannot be seen during electrochemical characterization of the system.

While all used electrodes are reportedly stable in acidic and alkaline conditions, the general decrease of yield with KOH at room temperature indicates a lower activity of used catalysts in alkaline media compared to the acidic H_2SO_4 solution. In contrast to the results using H_2SO_4, only Pt (2.10 V vs. RHE, according to CV) results in detectable formation of acetaldehyde while RuO_2 and $(Ru_{0.75}:Ti_{0.25})O_2$ (1.42 V vs. RHE, according to CV) show a selective production of acetic acid. The observed selectivity towards acetic acid formation indicates a promotion of consecutive readsorption and oxidation of acetaldehyde to acetic acid in KOH for RuO_2-based electrodes in addition to the direct oxidation of ethanol to acetic acid. The highest yield is again provided by RuO_2 on Ti with 12±0% for acetic acid. 8±3% are obtained using $(Ru_{0.75}:Ti_{0.25})O_2$. Here, the trend in yield matches the ECSA results, indicating that a higher active surface leads to higher yields. Pt results in a yield of 3±1% for acetic acid and 1±0% for acetaldehyde. In contrast, *FE* using Pt decreases vastly to 16±2% using KOH probably resulting from increased OER. The *FE* of $(Ru_{0.75}:Ti_{0.25})O_2$ decreases from 121±12% to 94±10% indicating increased CO_2 formation. For RuO_2, a high *FE* is obtained. The blank experiments with H_2SO_4 described above were repeated using KOH solution. Results showed a formation of acetic acid from acetaldehyde without applying current in alkaline solution. Using ethanol under similar conditions did not result in the consumption of ethanol. In summary, while higher yields and *FE* were obtained using H_2SO_4, acetic acid was produced as main product in alkaline solution using RuO_2.

Next, the influence of reaction conditions was further investigated by increasing the temperature to 60 °C (Figure 6). Although H_2SO_4 showed more promising results at room temperature, experiments at 60 °C were conducted using KOH, because electrodes based on RuO_2 showed a degradation of the coating layer in acidic media during electrolysis experiments at elevated temperatures. As Kim *et al.* report a high stability of RuO_2, this is most likely caused by the manufacturing procedure of the electrode coating which has to be investigated further.[16]

The reaction time had to be increased to 7.5 h to ensure suitable conversion in a larger cell used for experiments at increased temperature. Faraday equivalents (F_{eq}) (referred to acetic acid) varied between 0.15 and 0.44 as the reaction was conducted using a fixed reaction time, allowing for maximum yield between 15% and 44%. All electrode materials show a significant improvement of yield compared to the reaction at room temperature. The largest improvement can be seen for electrodes based on RuO_2. Similar to the reaction at room temperature using KOH, RuO_2-based catalysts led to a selective formation of acetic acid (29±2% (RuO_2)) and 26±2% yield ($(Ru_{0.75}:Ti_{0.25})O_2$). A condenser was utilized to achieve high carbon balances by inhibiting ethanol evaporation. Additionally, high carbon balances could be achieved throughout the reaction as surface oxidants (O, OH) are reported to inhibit the C–C bond cleavage towards CO_2.[28] Comparing reactions at room temperature and at 60 °C, *FE* increases to 74±0% using Pt. RuO_2-based catalysts showed a different behavior, where the *FE* of RuO_2 decreased to 71±7%, while *FE* for $(Ru_{0.75}:Ti_{0.25})O_2$ stayed constant at 88±0%. A possible explanation might be that in case of RuO_2 OER strongly increases at 60 °C (Figure S 7) due to a decreased onset potential compared to room temperature while the onset of ethanol oxidation stays similar. In case of Pt, while OER onset decreases, ethanol oxidation onset also decreases drastically, leading to an increase in *FE*. $(Ru_{0.75}:Ti_{0.25})O_2$ reaches similar onset potentials at both room temperature and 60 °C. Additionally, in case of $(Ru_{0.75}:Ti_{0.25})O_2$, constant *FE* indicates a partially OER-inhibiting effect of TiO_2 as was previously reported in literature.[22] Higher catalyst activity was observed at an increased temperature of 60 °C, however, the activity towards OER increased as well.

As higher potentials influence product selectivity and *FE* but also lead to desirable higher current densities, the applied potential was increased to 1.42 V vs. RHE and 1.45 V vs. RHE (Figure 5). The experiment was carried out using $(Ru_{0.75}:Ti_{0.25})O_2$ on Ti at 60 °C. For better comparison of the influence of the potential, a reaction cut-off was added at 0.15 F_{eq} (referred to acetic acid) instead of a fixed reaction time, allowing for a

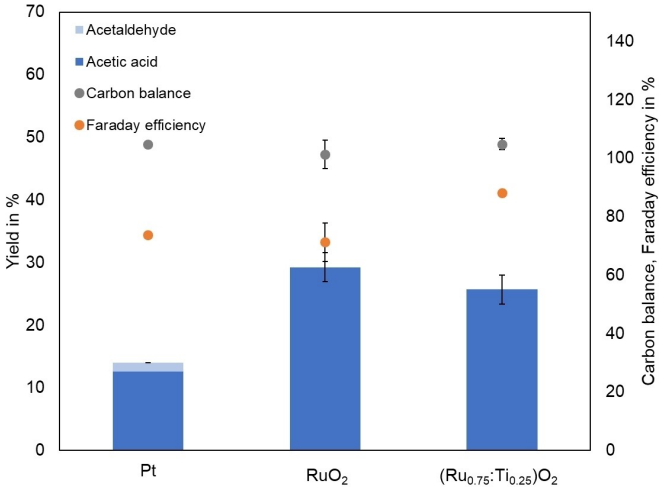

Figure 5. Yield, carbon balance and Faraday efficiency using Pt, RuO_2 on Ti and $(Ru_{0.75}:Ti_{0.25})O_2$ on Ti as catalyst for electrochemical ethanol oxidation of 0.1 M ethanol in 1 M KOH at 60 °C for 7.5 h at 2.1 V vs. RHE (Pt) and 1.4 V vs. RHE (RuO_2-based).

maximum yield of 15%. Figure 5 shows a decrease of the obtained yield by 1% (1.42 V vs. RHE) and 7% (1.45 V vs. RHE) which can be explained by an increasing O_2 formation at higher potentials because of a shift from ethanol oxidation towards OER. At a reaction potential of 1.45 V vs. RHE, the formation of acetaldehyde as additional reaction product to acetic acid is observed. This might be caused by enhanced OER partially inhibiting the additional oxidation step towards acetic acid due to adsorption on active sites.[28] The carbon balance increases with higher potentials from 98±3% to 100±1%, while *FE* decreases from 95±3% to 56±1%. Both results could again be attributed to an increased OER, which leads to blocked active sites on the electrode surface, reducing ethanol oxidation.

The experiment was repeated using $(Ru_{0.5}:Ti_{0.5})O_2$ on Ti to further investigate the influence of TiO_2 doping in electrodes on ethanol oxidation and OER that occurred during the experiment at elevated temperature of 60 °C (Figure 6). Here, a higher *FE* was observed for $(Ru_{0.75}:Ti_{0.25})O_2$ in comparison to RuO_2 showing clearly that the addition of higher amounts of TiO_2 holds a positive effect on the partially inhibition of OER. Improved product yields, shown in Figure 6, obtained using $(Ru_{0.5}:Ti_{0.5})O_2$ compared to $(Ru_{0.75}:Ti_{0.25})O_2$ are a direct result of the partially OER-inhibiting effect of TiO_2. The acetic acid yield stays nearly constant at around 18% between 1.40 V vs. RHE and 1.42 V vs. RHE. When increasing the potential to 1.45 V vs. RHE, the yield decreases to 11±1%. During the experiment using 1.40 V vs. RHE, less than 1% acetaldehyde and otherwise only acetic acid was formed. The formation of acetaldehyde implies a connection to the lower amount of active centers on the electrode surface compared to $(Ru_{0.75}:Ti_{0.25})O_2$ resulting in lower overall conversion. The carbon balance stays constant at around 100%, matching the expectations as low amounts of CO_2 formation were observed during prior experiments at elevated temperatures. In summary, increasing the reaction potential leads to an increasing concurrence of OER on the ethanol oxidation. The addition of TiO_2 can decrease the concurrence of OER due to a partially OER-inhibiting effect.

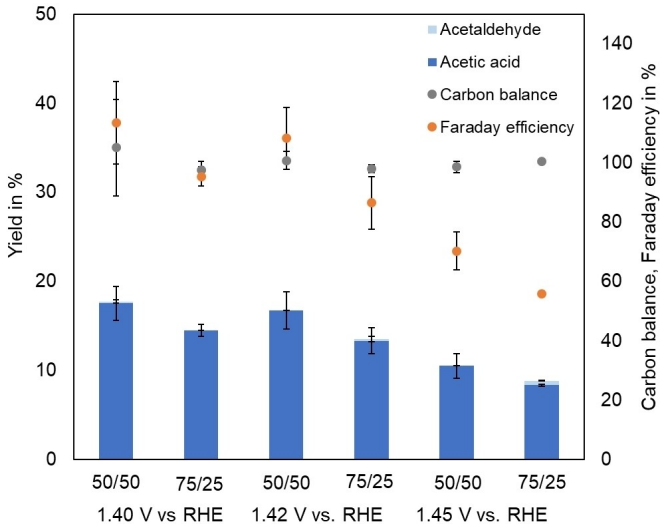

Figure 6. Yield, carbon balance and Faraday efficiency using $(Ru_{0.75}:Ti_{0.25})O_2$ on Ti (75/25) and $(Ru_{0.5}:Ti_{0.5})O_2$ on Ti (50/50) as catalyst for electrochemical ethanol oxidation of 0.1 M ethanol in 1 M KOH. The reaction was conducted at 60 °C at potentials of 1.40 V vs. RHE, 1.42 V vs. RHE and 1.45 V vs. RHE until a charge of 150 C was reached.

In the following part, practical aspects regarding ethanol oxidation were studied. To investigate the possibility of a continuous reaction, electrolysis was conducted using a semi-batch reaction setup. The electrolysis was performed under galvanostatic reaction conditions at 10 mA using $(Ru_{0.75}:Ti_{0.25})O_2$ on Ti, eliminating the need of an additional reference electrode. $(Ru_{0.75}:Ti_{0.25})O_2$ on Ti was chosen in contrast to other tested catalysts in an effort to keep the conductivity at 10 mA as high as possible, allowing for low reaction potentials, while still being able to utilize the partially OER inhibiting properties of TiO_2. The experiment was carried out at a temperature of 60 °C, utilizing a flow rate of 1 mL·min^{-1}. As a semi-batch reaction system was used, the electrolyte solution passed through the reactor multiple times, increasing the overall reaction time of the solution compared to a single-pass flow cell. In semi-batch experiments, 0.55 F_{eq} were applied with respect to acetic acid, theoretically allowing for a maximum yield of 55% within the reaction time of 3 h. The semi-batch experiment showed a yield of of 23±1% after 3 h which equals a *FE* of only 39±1%. In comparison to the batch experiment at 0.15 F_{eq}, these results are quite low as the batch experiment reached yields of up to 15±1% and therefore *FE* of 97±3%, indicating an increased OER at higher reaction potentials. Similar to most batch experiments in KOH, acetic acid was the only liquid product received during the semi-batch reaction. The carbon balance of 86±2% implies either formation of CO_2 or evaporation of ethanol during the reaction. Contrasting to batch experiments, no condenser can be installed in the used semi-batch setup.

Since the energy consumption of a reaction is of high industrial importance, the energy demand per kg of H_2 of both ethanol oxidation and OER was calculated at 40 mA (Equation 10–12). The energy demand of the electrochemical ethanol oxidation was calculated to have a higher energy demand per kg of H_2 of 60.8 kWh·kg^{-1} compared to 58.3 kWh·kg^{-1} for OER using $(Ru_{0.5}:Ti_{0.5})O_2$ on Ti. This is surprising considering that according to CV data (Figure S 3–6) ethanol oxidation shows a lower oxidation potential compared to OER. The results can be explained by OER dominating over ethanol oxidation at 40 mA (Supporting information, Figure S 9). $(Ru_{0.5}:Ti_{0.5})O_2$ on Ti was used as switchable catalyst as prior experiments showed an partially inhibition of OER during ethanol oxidation, leading to better conversion rates, while still enabling sufficient oxygen evolution during OER cycles. Based on those results, we concluded that cycling between anode reactions like ethanol oxidation and OER adjusting for the dynamic costs of energy could be favorable for industry purposes. At low cost of energy, OER can optimize energy usage for H_2 production, while value-adding products formed by ethanol oxidation could be produced at higher cost of energy. The procedure, called anodic oxidation cycling in the following, is described closer in the experimental section. As a first experiment, anodic oxidation cycling was repeated 6 times switching between ethanol oxidation and OER every 30 min at 40 mA (Figure S 10–11). Results show lower cell potentials for OER compared to ethanol

oxidation and an overall trend of constantly increasing cell potentials from cycle to cycle. While the increase in cell potential indicates a slight decrease in electrode activity over the experiment, the catalyst still performs well in OER and EOR. Additionally, the results indicate robustness towards switching the reactions, introducing an interesting concept that offers potential for future implementation.

Conclusions

In this work, electrochemical ethanol oxidation was investigated in applied electrosynthesis as an alternative to OER for efficient H_2 production using well-established catalysts like Pt and RuO_2-based materials. Experiments using RuO_2 show selective formation of acetic acid in alkaline electrolyte solution at 60 °C with yields of up to 29% at 71% *FE* at 1.40 V vs. RHE. An increase of reaction potential to 1.45 V vs. RHE showed a decrease in *FE* of the value-added products to 56% ($(Ru_{0.75}:Ti_{0.25})O_2$). It was suggested that an increase of OER leads to blocking of active catalyst sites due to adsorption decreasing the conversion rate of ethanol and acetaldehyde. Increasing the TiO_2 content of RuO_2-based electrodes showed a partially OER-inhibiting effect and therefore an increase of *FE* for organic value-added products compared to RuO_2 electrodes. Anodic oxidation cycling was introduced as a novel method for cost optimization. $(Ru_{0.5}:Ti_{0.5})O_2$ on Ti can be applied when cycling reactions according to their energy demand. This process reduces cost of H_2 production by enabling production of value-added products to compensate for high electricity prices and allow for efficient OER at low energy prices.

Experimental Section

Materials: Electrolyte solutions were prepared using Milli-Q water. All chemicals besides acetaldehyde (Fluka), $RuCl_3$ (anhydrous, abcr) and $TiCl_3$ (15% in 10% HCl, Merck) were purchased from Chemsolute. Chemicals were used without further preparation. Electrochemical cells were custom build (cell A: diameter: 2 cm, thickness: 1 cm; cell B: diameter: 4 cm, thickness: 2 cm, with ice-cooled condenser) and could be operated with a mgw Lauda M3 thermostat (anode side).[29]

Characterization: Electrolysis experiments were evaluated using HPLC (Shimadzu Prominence LC-20 system) with a reflective index detector and a CS organic acid resin column. Samples were eluted at 40 °C with a mixture of trifluoroacetic acid (TFA) in water (154 $\mu L \cdot L^{-1}$) using a flow rate of 1 $mL \cdot min^{-1}$.

Electrode preparation: Ti electrodes (5 cm×5 cm) were cut, sanded with 400 grid sandpaper and cleaned using water and acetone. The catalyst solutions were prepared according to Näslund *et al.*[15] RuCl3 (1.0375 g, $5 \cdot 10^{-3}$ mol) was mixed with 10% HCl in water (4.72 mL) and isopropanol (0.23 mL). $TiCl_3$ stock solution was prepared by mixing $TiCl_3$ 15% in 10% HCl in water (4.72 mL) with isopropanol (0.23 mL). Both stock solutions were sonicated for 5 min before use. The coating solutions were combined according to the needed ratio by mixing them 2:1 with isopropanol and sonicated for 5 min. The solution was vortexed for 30 s before evenly coating the electrodes. Electrodes were dried in an oven at 80 °C for 15 min before calcinating in a muffle oven for 15 min at 470 °C with a heating rate of 20 $K \cdot min^{-1}$. The coating process was repeated additional two times, increasing the calcination time to 2 h in the last step.

Cyclic Voltammetry: CVs were recorded in a three-electrode arrangement in a glass vial using 0.5 M H_2SO_4 or KOH as electrolyte solution and 1 M ethanol. Reference experiments were performed without substrate. While the working electrode was varied, Pt was used as counter electrode in all experiments. The reference electrode was either Ag/AgCl in 3 M KCl or Hg/HgO in 1 M KOH according to the pH of the electrolyte solution. All measurements were carried out at a scan rate of 10 $mV \cdot s^{-1}$ for three scans at either room temperature or 60 °C.

Impedance, Tafel and double layer capacity analysis: Electrochemical data for electrode characterization were recorded in a three-electrode arrangement in a glass vial using 1 M H_2SO_4 or KOH as electrolyte solution without ethanol. While the working electrode was varied, Pt was used as counter electrode in all experiments. The reference electrode was either Ag/AgCl in 3 M KCl or Hg/HgO in 1 M KOH according to the pH of the electrolyte solution. All measurements were carried out room temperature.

Electrosynthesis: Electrolysis experiments were conducted using either 1 M H_2SO_4 or 1 M KOH with 0.1 M ethanol. pH experiments were performed in cell A at room temperature, while all batch experiments at 60 °C used cell B. Potential were set to 1.72 V vs. RHE (Pt) and 1.42 V vs. RHE (RuO_2-based) in H_2SO_4 and 2.10 V vs. RHE (Pt) and 1.40 V vs. RHE (RuO_2-based) in KOH. Semi-batch experiments were performed at 60 °C at 10 mA using cell A in combination with a HPLC pump.

Anodic Oxidation Cycling: Cell A was combined with a cathode compartment of similar size, separated by a Nafion N-324 membrane (0.15 mm, Teflon fabric reinforced) and heated to 60 °C using a thermostat. Ethanol oxidation and OER were performed at 40 mA using $(Ru_{0.5}:Ti_{0.5})O_2$ on Ti alternating every 30 min for six hours total. The cell was flushed twice between ethanol oxidation and OER using electrolyte. The anode compartment solution was alternated at 40 mA between 0.1 M ethanol in 1 M KOH (ethanol oxidation) and 1 M KOH (OER). The cathode compartment was always filled with 1 M KOH

Acknowledgements

This work was funded by the Federal Ministry of Education and Research within Hydrogen Cluster4Future (HylnnoSep - FKZ: 03ZU1115CA) as well as the Cluster of Excellence Fuel Science Center (EXC 2186, ID: 390919832) funded by the Excellence Initiative by the German federal and state governments to promote science and research at German universities. Open Access funding enabled and organized by Projekt DEAL.

Conflict of Interests

The authors declare no conflict of interest.

Data Availability Statement

The data that support the findings of this study are available from the corresponding author upon reasonable request.

Keywords: Electrochemistry · Electrochemical Ethanol Oxidation · Electrosynthesis · Water Splitting

[1] a) S. Ould Amrouche, D. Rekioua, T. Rekioua, S. Bacha, *Int. J. Hydrogen Energy* **2016**, *41*, 20914; b) S. R. Sinsel, R. L. Riemke, V. H. Hoffmann, *Renewable Energy* **2020**, *145*, 2271.
[2] M. Xiang, N. Wang, Z. Xu, H. Zhang, Z. Yan, *ChemPlusChem* **2021**, *86*, 1307.
[3] A. L. Santos, M.-J. Cebola, D. M. F. Santos, *Energies* **2021**, *14*.
[4] B. You, G. Han, Y. Sun, *Chem. Commun.* **2018**, *54*, 5943.
[5] D. Yan, C. Mebrahtu, S. Wang, R. Palkovits, *Angew. Chem.* **2022**.
[6] W. M. Haynes (Ed.) *CRC handbook of chemistry and physics. A ready-reference book of chemical and physical data*, CRC Press, Boca Raton, London, New York, **2017**.
[7] a) R. A. Weusthuis, J. M. Aarts, J. P. Sanders, *Biofuels Bioprod. Biorefin.* **2011**, *5*, 486; b) R. P. Brexó, A. S. Sant'Ana, *Renewable Sustainable Energy Rev.* **2017**, *73*, 423; c) S. González-García, M. T. Moreira, G. Feijoo, *Biofuels Bioprod. Biorefin.* **2010**, *4*, 118.
[8] a) H. Wang, Z. Jusys, R. J. Behm, *J. Phys. Chem. B* **2004**, *108*, 19413; b) N. Fujiwara, K. A. Friedrich, U. Stimming, *J. Electroanal. Chem.* **1999**, *472*, 120.
[9] M. Wala, W. Simka, *Molecules* **2021**, *26*, 2144.
[10] J. Bai, D. Liu, J. Yang, Y. Chen, *ChemSusChem* **2019**, *12*, 2117.
[11] a) X. Meng, Y. Ouyang, H. Wu, H. Huang, F. Wang, S. Wang, M. Jiang, L. Y. Zhang, *J. Colloid Interface Sci.* **2021**, *586*, 200; b) X. Meng, T. Zeng, S. Ma, L. Zheng, H. Chen, W. Yuan, L. Y. Zhang, *Adv. Mater. Interfaces* **2022**, *9*; c) T. Zeng, X. Meng, H. Huang, L. Zheng, H. Chen, Y. Zhang, W. Yuan, L. Y. Zhang, *Small* **2022**, *18*, e2107623.
[12] a) F. Colmati, G. Tremiliosi-Filho, E. R. Gonzalez, A. Berná, E. Herrero, J. M. Feliu, *Faraday Discuss.* **2009**, *140*, 379; b) V. Del Colle, J. Souza-Garcia, G. Tremiliosi-Filho, E. Herrero, J. M. Feliu, *Phys. Chem. Chem. Phys.* **2011**, *13*, 12163.
[13] R. M. Altarawneh, T. M. Brueckner, B. Chen, P. G. Pickup, *J. Power Sources* **2018**, *400*, 369.
[14] M. Mansor, S. N. Timmiati, K. L. Lim, W. Y. Wong, S. K. Kamarudin, N. H. Nazirah Kamarudin, *Int. J. Hydrogen Energy* **2019**, *44*, 14744.
[15] L. -Å Näslund, C. M. Sánchez-Sánchez, Á. S. Ingason, J. Bäckström, E. Herrero, J. Rosen, S. Holmin, *J. Phys. Chem.* **2013**, *117*, 6126.
[16] J.-W. Kim, S.-M. Park, *J. Electrochem. Soc.* **1999**, *146*, 1075.
[17] C.-C. Hu, K.-H. Chang, M.-C. Lin, Y.-T. Wu, *Nano Lett.* **2006**, *6*, 2690.
[18] P. Shrivastava, M. S. Moats, *J. Appl. Electrochem.* **2009**, *39*, 107.
[19] B. Hasa, E. Kalamaras, E. I. Papaioannou, L. Sygellou, A. Katsaounis, *Int. J. Hydrogen Energy* **2013**, *38*, 15395.
[20] a) H. Luo, J. Barrio, N. Sunny, A. Li, L. Steier, N. Shah, I. E. L. Stephens, M.-M. Titirici, *Adv. Energy Mater.* **2021**, *11*, 2101180; b) B. Sarmah, B. Satpati, R. Srivastava, *ACS Omega* **2018**, *3*, 7944.
[21] C. Tian, X.-Y. Li, V. E. Nelson, P. Ou, D. Zhou, Y. Chen, J. Zhang, J. E. Huang, N. Wang, J. Yu et al, *ACS Energy Lett.* **2023**, *8*, 4096–4103.
[22] J. C. Fornaciari, D. Primc, K. Kawashima, B. R. Wygant, S. Verma, L. Spanu, C. B. Mullins, A. T. Bell, A. Z. Weber, *ACS Energy Lett.* **2020**, *5*, 2954.
[23] C.-P. Lo, G. Wang, A. Kumar, V. Ramani, *Appl. Catal. B* **2013**, *140–141*, 133.
[24] L. Yu, J. Xi, *Electrochim. Acta* **2012**, *67*, 166.
[25] a) M. Berger, I. M. Popa, L. Negahdar, S. Palkovits, B. Kaufmann, M. Pilaski, H. Hoster, R. Palkovits, *ChemElectroChem* **2023**, *10*, e2023002; b) R. L. Doyle, M. E. G. Lyons, *J. Electrochem. Soc.* **2013**, *160*, H142–H154; c) L. Negahdar, F. Zeng, S. Palkovits, C. Broicher, R. Palkovits, *ChemElectroChem* **2019**, *6*, 5588.
[26] a) C. C. L. McCrory, S. Jung, J. C. Peters, T. F. Jaramillo, *J. Am. Chem. Soc.* **2013**, *135*, 16977; b) Y. Dang, T. Wu, H. Tan, J. Wang, C. Cui, P. Kerns, W. Zhao, L. Posada, L. Wen, S. L. Suib, *Energy Environ. Sci.* **2021**, *14*, 5433; c) C. Reiser, P. Keßler, M. Kamp, V. Jovic, S. Moser, *J. Phys. Chem. C* **2023**, *127*, 3682.
[27] W. Yong-gang, Z. Xiao-gang, *Electrochim. Acta* **2004**, *49*, 1957.
[28] R. Kavanagh, X.-M. Cao, W.-F. Lin, C. Hardacre, P. Hu, *Angew. Chem. Int. Ed.* **2012**, *51*, 1572.
[29] N. Kurig, J. Meyers, F. J. Holzhäuser, S. Palkovits, R. Palkovits, *ACS Sustainable Chem. Eng.* **2021**, *9*, 1229.

Manuscript received: December 4, 2023
Revised manuscript received: February 14, 2024
Version of record online: April 19, 2024